Supporting Information Corrected May 27, 2013

SUPPLEMENTARY INFORMATION APPENDIX

SI FIGURES

Fig. S1. Cartoon representation of the DV-E homodimer. The E-protein monomer has three domains, EDI (red), EDII (yellow) and EDIII (blue). The fusion loop located on EDII domain is colored in green; the A-strand epitope on EDIII domain is colored in magenta.

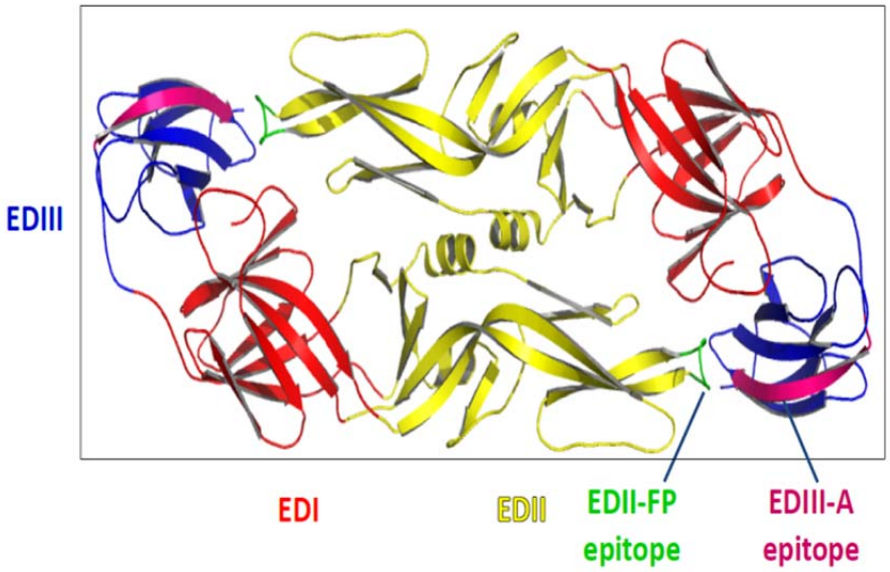

Fig. S2. *In vitro* activity determined by FRNT, with error bars representing standard deviation. Affinity values determined by competition ELISA.

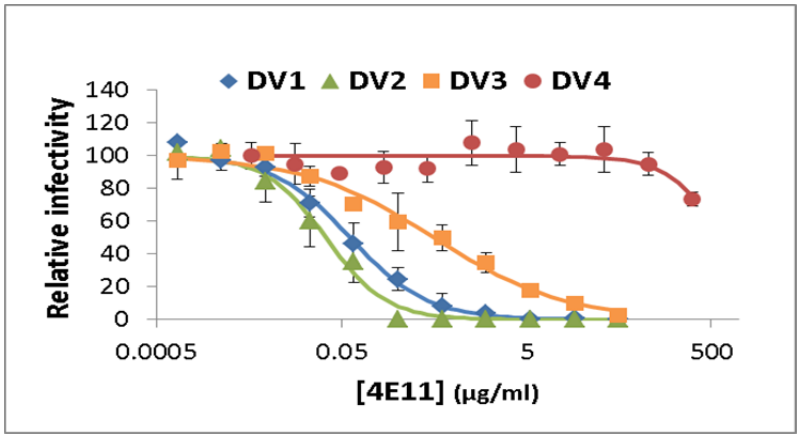

EDIII-DV1 K_D (nM)	EDIII-DV2 K_D (nM)	EDIII-DV3 K_D (nM)	EDIII-DV4 K_D (nM)
0.328	5.20	21.8	40,793

Fig. S3. Physicochemical determinants of protein-protein interaction.

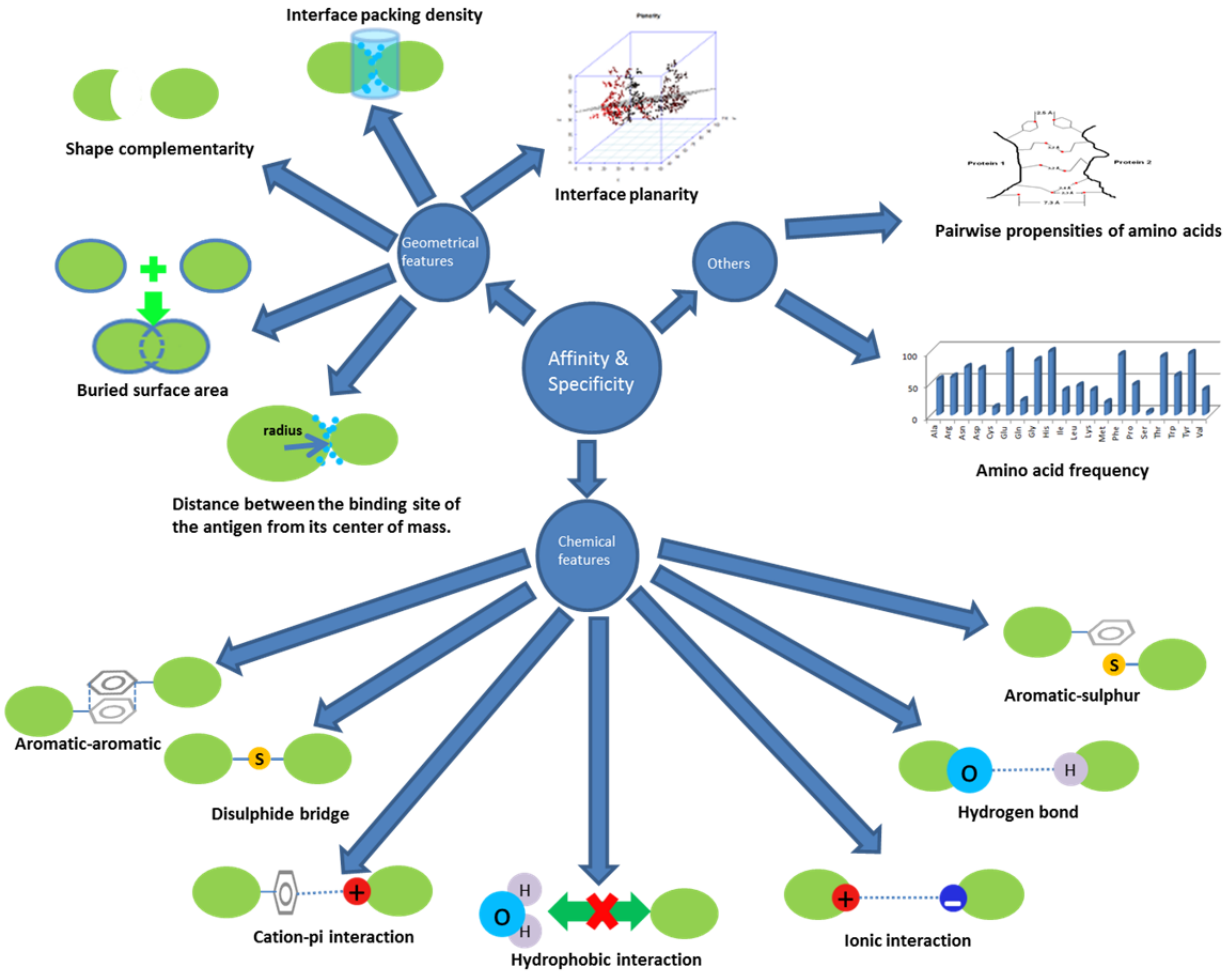

Fig. S4.Computer generated decoy models for PDB: 2B2X (antigen: integrin VLA1; antibody: Fab of AQC2 variant). Each point on the surface plot represents a docking decoy (one hundred decoys in total). The x-axis represents the ZRANK score; y-axis represents the ligand interface RMSD (in Å) to the crystal structure; z axis represents the MLR-based prediction probability. ZRANK scores of native-like structures vary between -60 to -30 Kcal/mol. The maximal ligand interface RMSD difference between structures having similar ZRANK scores (variation less than -3Kcal/mol) is 36 Å. The structure that received the lowest ZRANK score has ligand interface RMSD value of 40 Å. Using Pearson's correlation test, a significant positive linear relationship exists between MLR-based probability and RMSD (correlation coefficient: -0.25; p-value: 0.012). On the other hand, ZRANK does not have any linear correlation with RMSD (correlation coefficient: -0.01; p-value: 0.921) or MLR-probability (correlation coefficient: 0.1 and p-value: 0.3).

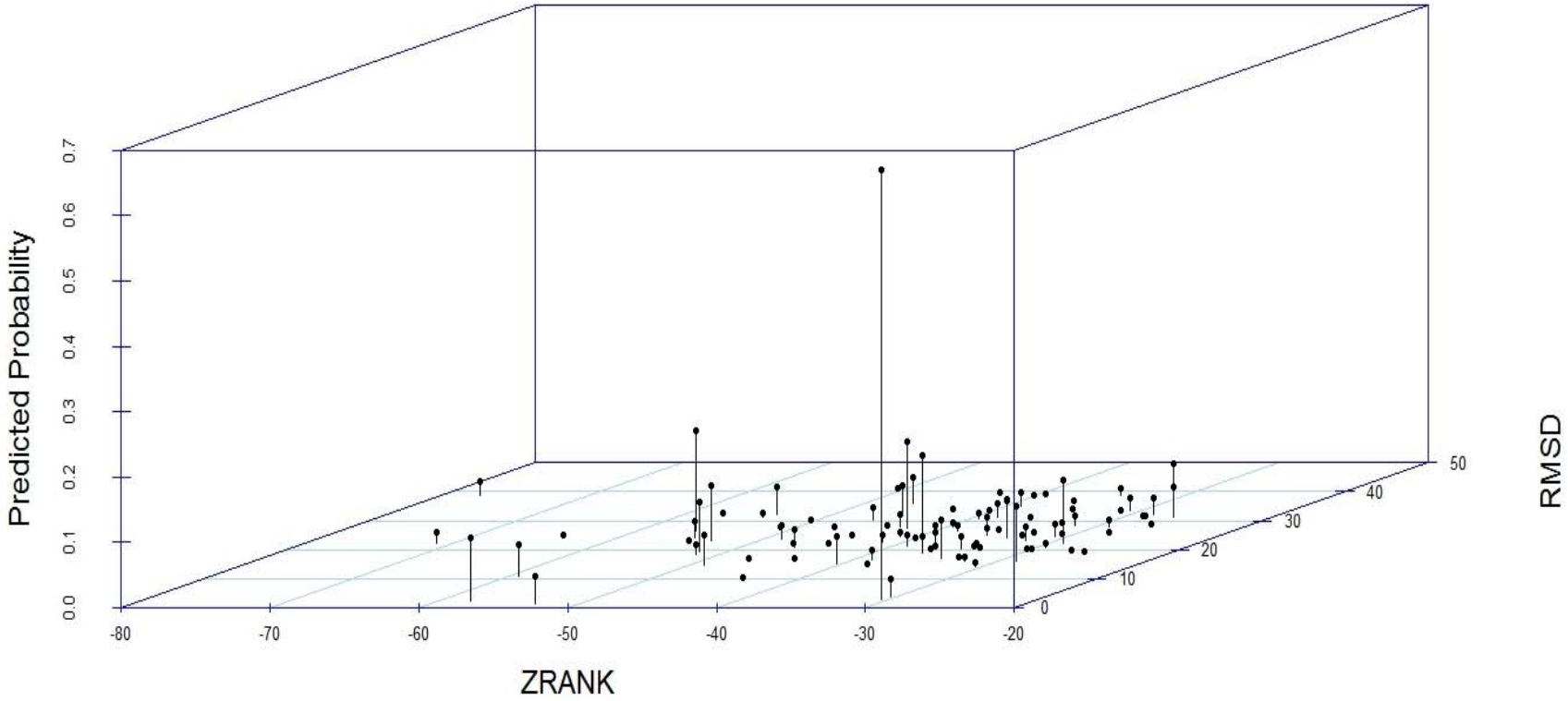

Fig. S5. Amino acid frequencies in paratope and epitope. Data generated from 84 antigen-antibody complexes.

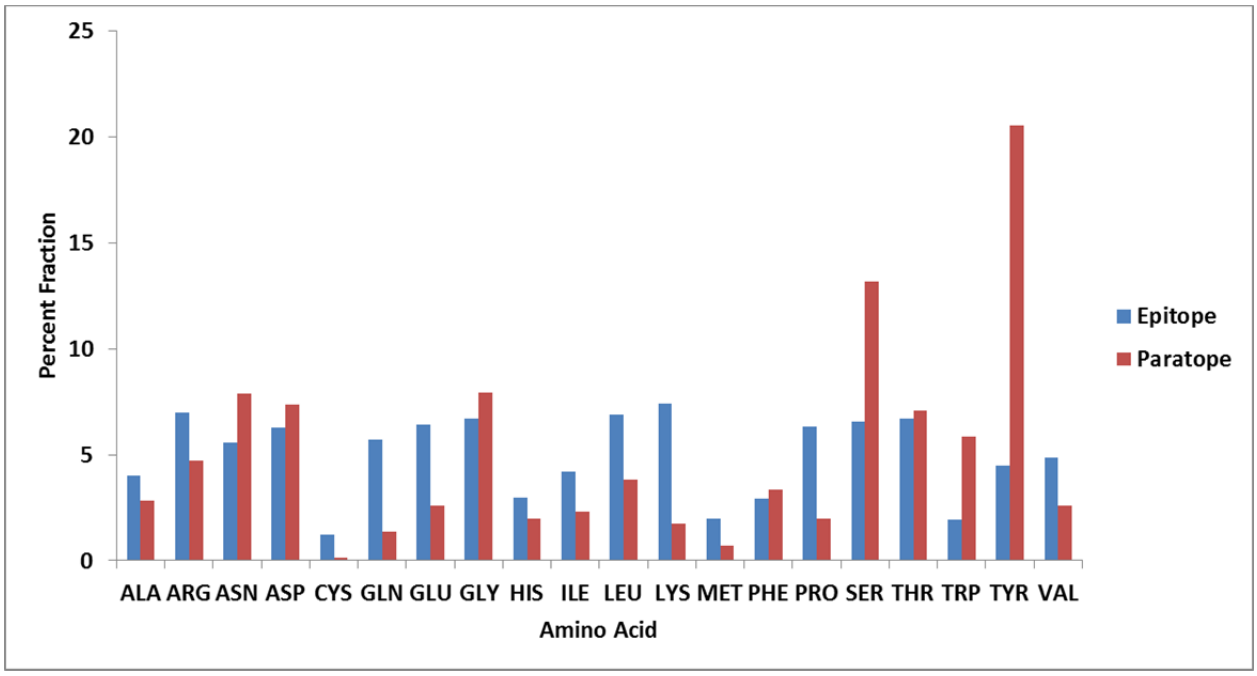

Fig. S6. Flowchart of the antibody design approach.

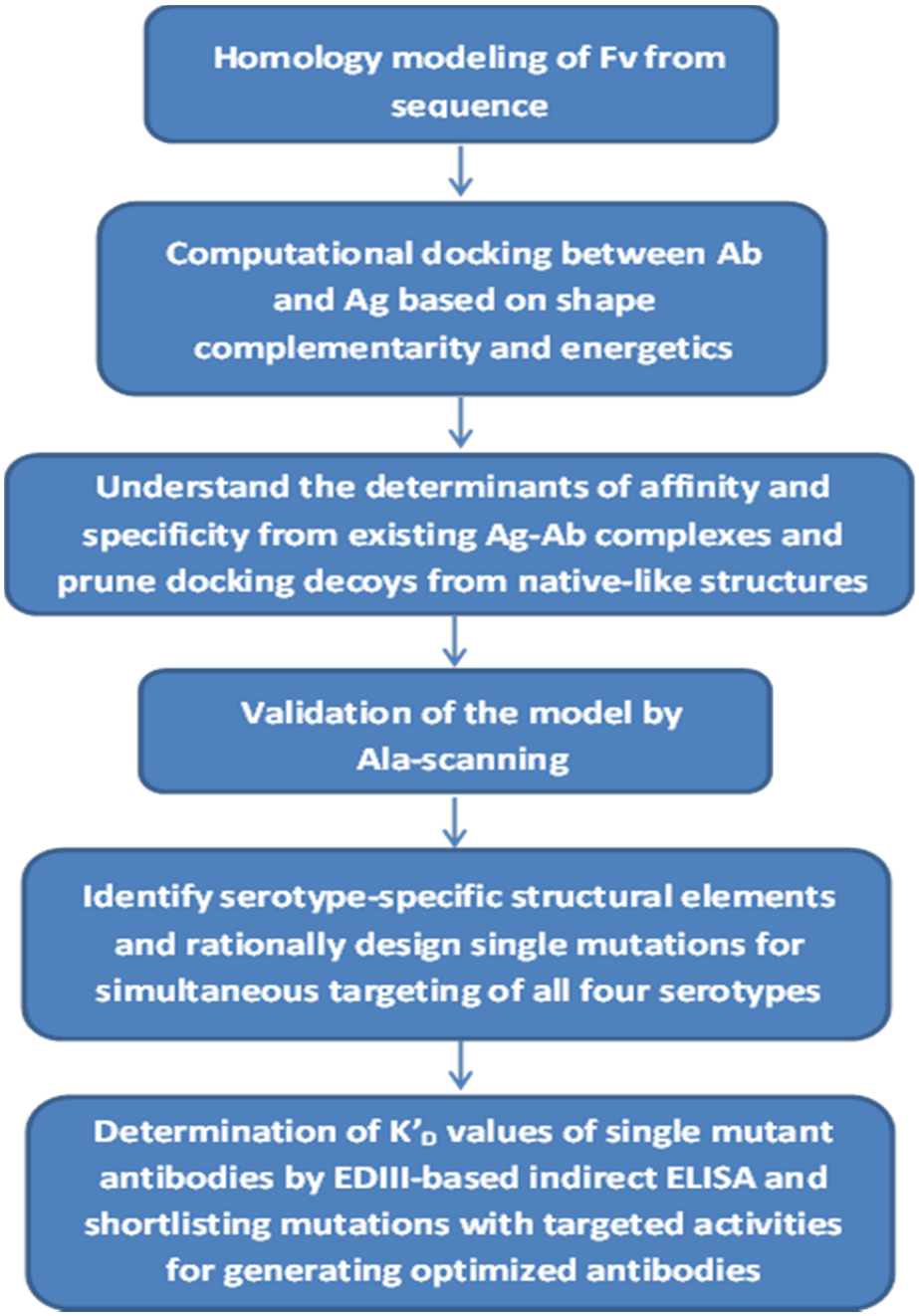

Fig. S7. Superposition of the top five docking models on fixed ED-III. ED-III is represented as spheres; 4E11, displayed as surface in each model, is colored differently, for clarity.

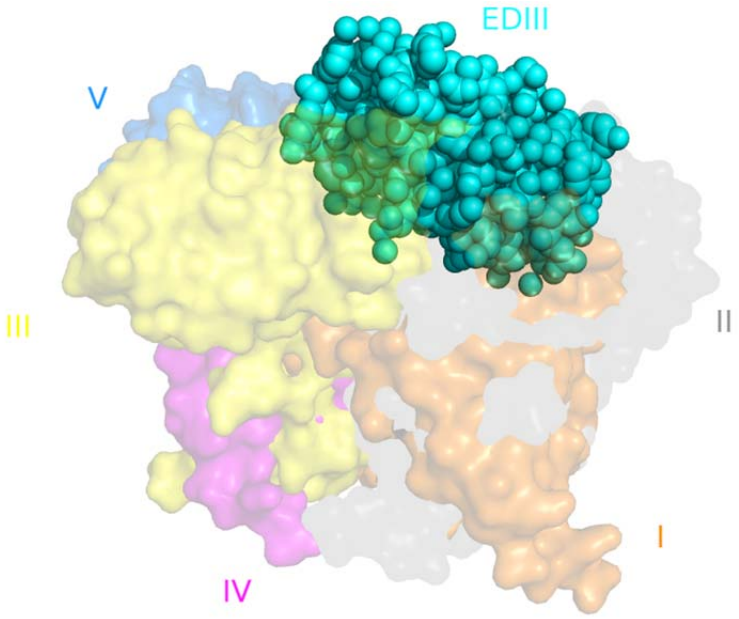

Fig. S8. Affinity-enhancing mutations localize to the periphery of the 4E11:EDIII-DV4 interface. The positive positions identified in the binding screen are highlighted (red) in a structural model of 4E11:EDIII-DV4 interaction. All successful mutations are located at the periphery of the binding interface. The two panels represent different views of the same model. EDIII, VH, and VL proteins are represented by blue, green, and yellow, respectively.

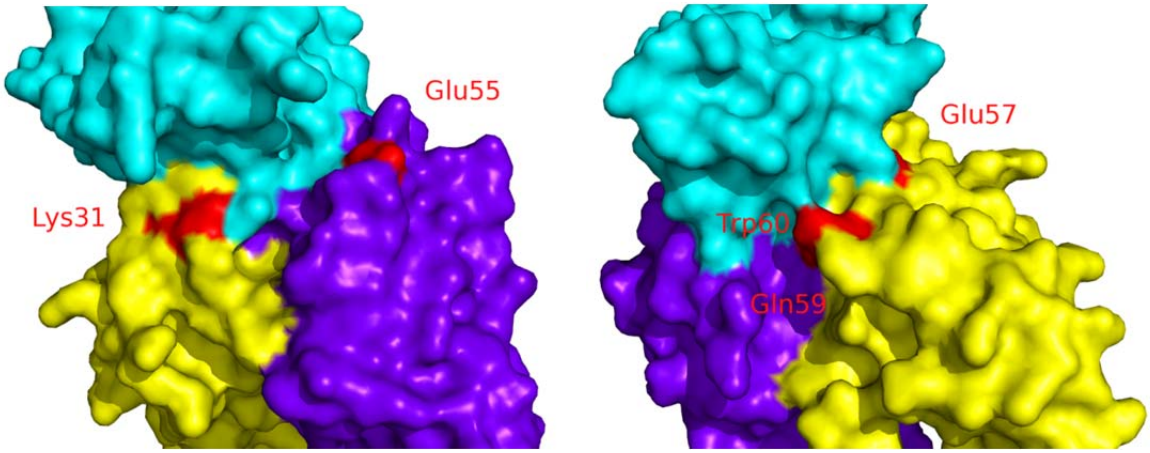

Fig. S9. SPR sensorgrams of 4E11 WT and 4E5A with antigens EDIII of DV1-4.

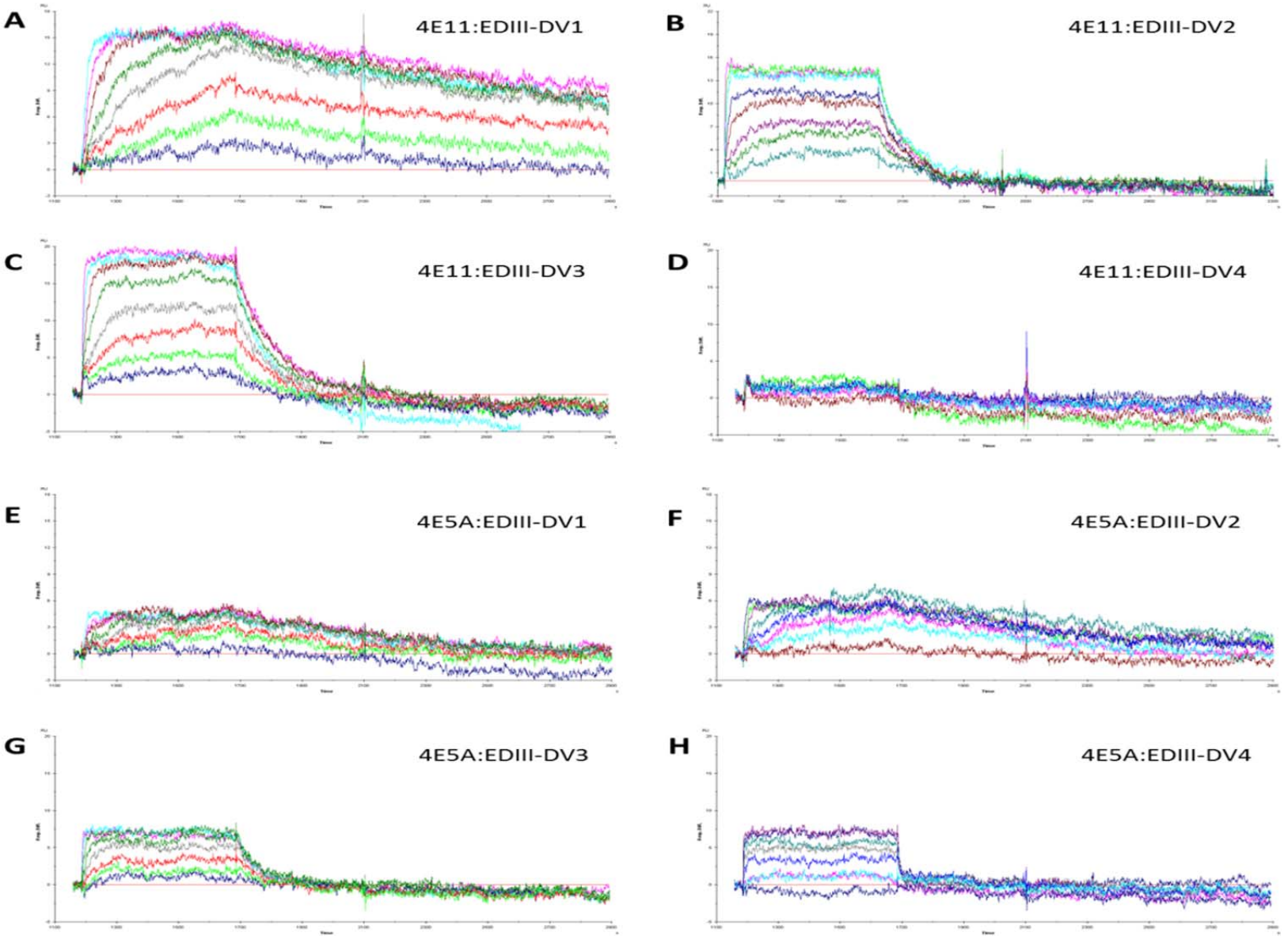

SI TABLES

Table S1. Description of physicochemical features.

Feature No.	Description of feature	Feature sub-classification/Additional note
Chemical		
1	Number of various types of interactions	(1) hydrophobic, (2) disulfide bridges, (3) hydrogen bond, (4) ionic interactions, (5) aromatic-aromatic, (6) aromatic-sulfur, (7) cation-pi
2	Density of each type of interactions (i.e. how many contacts of each type is observed on average per 100 square Å of the interface)	(1) hydrophobic, (2) disulfide bridges, (3) hydrogen bond, (4) ionic interactions, (5) aromatic-aromatic, (6) aromatic-sulfur, (7) cation-pi
3	Classification of hydrogen-bonds	(1) main chain - main chain, (2) main chain - side chain, (3) side chain - side chain
4	Number of hydrogen bonds that involve charged residues	
5	Composition of chemical groups	(1) polar, (2) neutral and (3) non-polar
6	ZEPII	Assesses the frequencies of favorable epitope-paratope inter-residue interactions to indicate the probability of antibody binding to a given surface
Physical		
7	Buried surface area	
8	Planarity	
9	Surface complementarity	
10	Interface atom packing density	
11	Distance between the binding site of the antigen from its center of mass	

Table S2. Training data set of antigen – antibody complexes (total number of complexes = 40).

Code	Name	Antigen-Antibody Complex	Antigen		Antibody	
			Chain(s)	Size	Chain(s)	Size
1F58	Igg1 Antibody 58.2 / Protein (Exterior Membrane Glycoprotein (gp 120)	Fab 58.2 W/ HIV-1 Gp120 Peptide	P	23	L,H	216,228
1OSP	Crystal Structure Of Outer Surface Protein A Of Borrelia Burgdorferi Complexed With A Murine Monoclonal Antibody Fab	Fab184.1/ Ospa_S84c	O	257	L,H	214,218
1BGX	Taq Polymerase In Complex With Tp7, An Inhibitory Fab	Fab Tp7/ Taq Dna Polymerase	T	832	L,H	210,213
1FE8	Crystal Structure Of The Von Willebrand Factor A3 Domain In Complex With A Fab Fragment Of Igg Ru5 That Inhibits Collagen Binding	Fab Ru5 W/ Vwf A3	A,B,C	196	L,M,N,H,I,J	210, 211
1NFD	An Alpha-Beta T Cell Receptor (Tcr) Heterodimer In Complex With An Anti-Tcr Fab Fragment Derived From A Mitogenic Antibody	Fab H57 W/ Tcr	B,D	239	L,H	212,222
1ORS	Membrane Protein X-Ray Structure Of The Kvap Potassium Channel Voltage Sensor In Complex With An Fab	Fab 33H1 W/Potassium Channel	C	132	A,B	214,221
1KB9	Yeast Cytochrome Bc1 Complex	Fv w/ ubiquinol-cytochrome c reductase iron-sulfur subunit	E	185	K,J	107,127
1AR1	Complex (Oxidoreductase/Antibody) Structure At 2.7 Angstrom Resolution Of The Paracoccus Denitrificans Two-Subunit Cytochrome C Oxidase Complexed With An Antibody Fv Fragment	Fv w/ cytochrome c oxidase	A,B	558,298	C,D	120,127

Code	Name	Antigen-Antibody Complex	Antigen		Antibody	
			Chain(s)	Size	Chain(s)	Size
1N8Z	Transferase Crystal Structure Of Extracellular Domain Of Human Her2 Complexed With Herceptin Fab	Fab Herceptin W/ Receptor Protein-Tyrosine Kinase Erbb-2	C	607	A,B	214,220
1RJL	Immune System Structure Of The Complex Between Ospb-Ct And Bactericidal Fab-H6831	Fab H6831 W/ Outer Surface Protein B	C	95	A,B	212,221
1TZI	Immune System Crystal Structure Of The Fab Yads2 Complexed With H-Vegf	Fab YADS2 W/ VEGF	V	102	A,B	242,222
1NL0	Immune System Crystal Structure Of Human Factor Ix Gla Domain In Complex Of An Inhibitory Antibody, 10c12	Fab 10C12 W/ Human Factor IX GLA Domain	G	51	L,H	213,224
1UAC	Immune System/Hydrolase Crystal Structure Of Hyhel-10 Fv Mutant Sfsf Complexed With Turkey White Lysozyme	Fv HYHEL-10 W/ Lysozyme	Y	129	L,H	107,114
1H0D	Immune System/Hydrolase Crystal Structure Of Human Angiogenin In Complex With Fab Fragment Of Its Monoclonal Antibody Mab 26-2f	Fab 26-2F W/ Angiogenin	C	123	A,B	216,223
1V7M	Immune System/Cytokine Human Thrombopoietin Functional Domain Complexed To Neutralizing Antibody Tn1 Fab	Fab TN1 W/ human thrombopoietin	V	163	L,H	213,217
1W72	Immune System Crystal Structure Of Hla-A1:Mage-A1 In Complex With Fab-Hyb3	Fab HYB3 W/ HLA-A1:MAGE-A1	A,C,D	274, 9, 274	L,H	210,223

Code	Name	Antigen-Antibody Complex	Antigen		Antibody	
	Chain(s)	Size	Chain(s)	Size		
1FNS	Crystal Structure Of The Von Willebrand Factor (Vwf) A1 Domain I546v Mutant In Complex With The Function Blocking Fab Nmc4	Fab Nmc-4 W/ Vwf A1 I546V	A	196	L,H	214,225
1NMB	The Structure Of A Complex Between The Nc10 Antibody And Influenza Virus Neuraminidase And Comparison With The Overlapping Binding Site Of The Nc41 Antibody	Fab Nc10 W/ Influenza Neuraminidase N9	N	470	L,H	109,122
1JPS	Crystal Structure Of Tissue Factor In Complex With Humanized Fab D3h44	Fab D3h44 W/ Tissue Factor	T	219	L,H	214,225
1OAZ	Ige Fv Spe7 Complexed With A Recombinant Thioredoxin	Fv Spe7 W/ Trx-Shear3_1-123	A	123	L,H	110,122
1WEJ	Igg1 Fab Fragment (Of E8 Antibody) Complexed With Horse Cytochrome C At 1.8 A Resolution	Fab E8 W/ Cytochrome C	F	105	L,H	214,223
1JRH	Antibody A6 / INTERFERON-GAMMA RECEPTOR	Fab A6 W/ Ifgammar Alpha	I	108	L,H	213,219
1BJ1	Fab Fragment / Vascular Endothelial Growth Factor	Fab Antivegf(Humanized) W/VEGF	V,W	102	L,J,H,K	214,231
1FDL	Igg1-Kappa D1.3 Fab / Hen Egg White Lysozyme	Fab D1.3 W/ HEL	Y	129	L,H	214,218
1MLC	Igg1-Kappa D44.1 / Hen Egg White Lysozyme	Fab D44.1 W/HEL	E,F	129	A,C,B,D	214,218
1P2C	Light Chain Anti-Lysozyme Antibody F10.6.6 / Heavy Chain Vh+Ch1 Anti-Lysozyme Antibody F10.6.6 / Lysozyme C	Fab F10.6.6.(Affinity Maturation Of D44.1) W/HEL	C,F	129	A,D,B,E	212,218
1FBI	Igg1 F9.13.7 Fab / Guinea Fowl Lysozyme	Fab F9.13.7 W/ GEL (Guinea Fowl)	X,Y	129	L,P,H,Q	214,221

Code	Name	Antigen-Antibody Complex	Antigen		Antibody	
	Chain(s)	Size	Chain(s)	Size		
1BQL	Hyhel-5 Fab / Bobwhite Quail Lysozyme	Fab Hyhel-5 W/ BWQL (Bobwhite Quail Lysozyme)	Y	129	L,H	212,215
1DQJ	Anti-Lysozyme Antibody Hyhel-63 / Lysozyme	Fab Hyhel-63 W/ HEL	C	129	A,B	214,210
1JHL	Igg1-Kappa D11.15 Fv / Pheasant Egg White Lysozyme	Fv D11.15 W/PEL (Pheasant Egg White Lysozyme Heteroclitic W/HEL))	A	129	L,H	108,116
1C08	Anti-Hen Egg White Lysozyme Antibody (Hyhel -10) / Lysozyme	Fv Hyhel-10 W/ HEL	C	129	A,B	107,114
1BVK	Hulys11 / Lysozyme	Fv(Hu) D1.3 W/ HEL	C,F	129	A,D,B,E	108,117
1E6J	Immunoglobulin / CAPSID PROTEIN P24	Fab 13B5 W/ HIV-1 P24	P	210	L,H	210,219
1A2Y	Hen Egg White Lysozyme, D18A Mutant, In Complex With Mouse Monoclonal Antibody D1.3	Fv D1.3 W/ Hen Egg White Lysozyme Mutant	C	129	A, B	107,116
1EGJ	Immune System Domain 4 Of The Beta Common Chain In Complex With An Antibody	Fab BION-1 W/ IL-5 Receptor	A	101	L,H	215,220
1LK3	Interlukin-10 / 9D7	Fab 9D7 W/ IL-10(Hu)	A,B	160	L,M,H,I	210,219
1EO8	Influenza Virus Hemagglutinin Complexed With A Neutralizing Antibody	Fab BH151 W/ Hemagglutinin 9HA1 & HA2 Chains)	A,B	328, 175	L, H	210,217
1ADQ	Igg4 Rea Fc / Igm-Lambda Rf-An Fab	Fab Igmrhf W/ Fc	A	206	L,H	213,225
1QFU	Protein (Hemagglutinin (Ha1 Chain)) / Protein (Immunoglublin Igg1-Kappa Antibody Light & Heavy Chain)	Fab NC10 W/ Infuenza Hemaglutinin	A,B	328, 184	L,H	217,223
1NMC	Neuraminidase / Single Chain Antibody	Scfv NC10 W/ Infuenza Virus Neuraminidase	A,N	388	B,H,C,L	122,190

Table S3. Testing data set of antigen – antibody complexes (total number of complexes = 44).

Code	Name	Additional Info	Antigen	Antibody		
			Chain(s)	Size	Chain(s)	Size
2BDN	Small Inducible Cytokine A2 / Antibody Light & Heavy Chain 11k2	Fab 11K2 W/MCP-1	A	76	L,H	214, 217
2R69	Major Envelope Protein E / Light & Heavy Chain Of 1A1D-2	Fab 1A1D-2 W/ Dengue Virus E-DIII	A	97	L,H	212, 214
1ZTX	Envelope Protein / Heavy & Light Chain Of E16 Antibody	Fab E16 W/Wnilevirus Protein DIII	E	108	L,H	212, 219
1YQV	Hyhel-5 Antibody Light & Heavy Chain / Hen Egg White Lysozyme	Fab Hyhel-5 W/ HEL	Y	129	L,H	211, 215
2JEL	Jel42 Fab Fragment / Histidine-Containing Protein	Fab JEL42 W/Hpr (PEP:Phosphotransferase)	P	85	L,H	217, 218
2Q8B	Apical Membrane Antigen 1 / 1f9 Light & Heavy Chain	Fab 1F9 W/ AMA1(Malaria Antigen)	A	336	L,H	214, 210
2R0K	Poly(A)-Specific Ribonuclease	Fab 58 W/ HGFA	A	283	L,H	214, 225
2B2X	Integrin Alpha-1 / Antibody Aqc2 Fab Heavy & Light Chain	Fab ACQ W/ Integrin-Alpha-1 (VLA1)	A,B	223	H.I,L,M	226, 213
2NY7	Envelope Glycoprotein GP120 / T-Cell Surface Glycoprotein CD4 / Antibody 17B Light & Heavy Chain	Fab B12 W/ HIV-1 Gp120	G	317	L,H	215, 230

Code	Name	Additional Info	Antigen	Antibody		
			Chain(s)	Size	Chain(s)	Size
2J4W	Apical Membrane Antigen 1 / FAB Fragment Of Monoclonal Antibody F8.12.19	Fab F8.12.19 W/ Plasmodium Vivax Membrane Ag	D	445	L,H	213, 225
2DD8	Igg Heavy & Light Chain / Spike Glycoprotein	Fab M396 W/SARS-Cov Spike RBD	S	202	H,L	245, 213
2AEQ	Neuraminidase / Fab Light & Heavy Chain	Fab MEM5 W/ Influenza Neuraminidase	A	395	L,H	214, 217
2B4C	Envelope Glucoprotein / T-Cell Surface Glycoprotein Cd4 / Anti-Hiv-1 Gp120 Immunoglobulin X5 Light & Heavy Chain	Fab X5 W/ HIV-1 Gp120 V3	G, C	344, 181	L, H	215, 235
2UZI	Anti-Ras Fv Heavy & Light Chain / Gtpase Hras	Fv Anti-Ras W/ HRAS	R	166	L,H	114, 104
1XIW	T-Cell Surface Glycoprotein Cd3 Epsilon Chain, Delta Chain / Immunoglobulin Light & Heavy Chain Variable Region	Scfv UCHT1 W/ CD3e/D	A,E,B,F	105, 79	C,G, D,H	108, 122
3EO1	Structure Of The Fab Fragment Of Gc-1008 In Complex With Transforming Growth Factor-Beta 3	Fab GC1008 W/ transforming growth factor-beta 3	C	112	A,B	215,225
1YJD	Crystal Structure Of Human Cd28 In Complex With The Fab Fragment Of A Mitogenic Antibody (5.11a1)	Fab 5.11A1 W/ CD28	C	140	L,H	212,222
2FD6	Structure Of Human Urokinase Plasminogen Activator In Complex With Urokinase Receptor And An Anti-Upar Antibody At 1.9 A	Fab W/ Urokinase-Type Plasminogen Activator	A,U	276,122	L,H	214,213

Code	Name	Additional Info	Antigen	Antibody		
			Chain(s)	Size	Chain(s)	Size
3EOA	Crystal Structure The Fab Fragment Of Efalizumab In Complex With Lfa-1 I Domain, Form I	Fab EFALIZUMAB W/ LFA-1 I Domain,	J	181	L,H	214,220
2GHW	Crystal Structure Of Sars Spike Protein Receptor Binding Domain In Complex With A Neutralizing Antibody, 80r	Fab 80R W/ SARS Protein	A	203	B	247
2VXQ	Crystal Structure Of The Major Grass Pollen Allergen Phl P 2 In Complex With Its Specific Ige-Fab	Fab Ige W/ grass pollen allergen PHL P 2	A	96	L,H	214,216
3ETB	Crystal Structure Of The Engineered Neutralizing Antibody M18 Complexed With Anthrax Protective Antigen Domain 4	Fv M18 W/ Anthrax Protective Antigen	J	144	F	252
1YY9	Structure Of The Extracellular Domain Of The Epidermal Growth Factor Receptor In Complex With The Fab Fragment Of Cetuximab/Erbitux/Imc- C225	Fab CETUXIMAB W/ EGFR	A	624	C,D	213,221
2H9G	Crystal Structure Of Phage Derived Fab Bdf1 With Human Death Receptor 5 (Dr5)	FAB BDF1 W/ human death receptor 5 (	S	130	L,H	214,228
2VXS	Structure Of Il-17a In Complex With A Potent, Fully Human Neutralising Antibody	Fab CAT2200 W/ IL-17A	A	137	L,H	216,225
3FKU	Crystal Structure Of Influenza Hemagglutinin (H5) In Complex With A Broadly Neutralizing Antibody F10	Fv F10 W/ Influenza Hemagglutinin	E,F	338,182	X	280

Code	Name	Additional Info	Antigen	Antibody		
			Chain(s)	Size	Chain(s)	Size
2HFG	Crystal Structure Of Hbr3 Bound To Cb3s-Fab	Fab CB3S W/ HBR3	R	51	L,H	214,232
2VXT	Crystal Structure Of Human Il-18 Complexed To Murine Reference Antibody 125-2h Fab	Fab 125-2H W/ IL-18	I	157	L,H	214,216
2AEP	An Epidemiologically Significant Epitope Of A 1998 Influenza Virus Neuraminidase Forms A Highly Hydrated Interface In The Na-Antibody Complex.	Fab Mem5 W/ Influenza NA	A	395	L,H	214,217
2IH3	Ion Selectivity In A Semi-Synthetic K+ Channel Locked In The Conductive Conformation	Fab W/ Voltage-Gated Potassium Channel	C	122	B,A	212,219
2W9E	Structure Of Icsm 18 (Anti-Prp Therapeutic Antibody) Fab Fragment Complexed With Human Prp Fragment 119-231	ICSM 18-Anti-Prp Fab W/ Human Prion Protein	A	113	L,H	212,215
3G6D	Crystal Structure Of The Complex Between Cnto607 Fab And Il-13	Fab CNTO607 W/ IL-13	A	113	L,H	213,229
2ZJS	Crystal Structure Of Secye Translocon From Thermus Thermophilus With A Fab Fragment	Fab Anti-Secy W/ Secye Translocon	E,Y	60,434	L,H	214,221
3GI9	Crystal Structure Of Apct Transporter Bound To 7f11 Monoclonal Fab Fragment	Fab 7F11 W/ APCT Transporter	C	444	L,H	220,223
2ZUQ	Crystal Structure Of Dsbb-Fab Complex	Fab W/ Disulfide Bond Formation Protein B	A	176	B,C	239,221
3GRW	FGFR3 In Complex With A Fab	Fab R3Mab W/ FGFR3	A	241	L,H	214,235

Code	Name	Additional Info	Antigen	Antibody		
			Chain(s)	Size	Chain(s)	Size
3B9K	Crystal Structure Of Cd8alpha-Beta In Complex With Yts 156.7 Fab	Fab YTS156.7 W/ CD8ALPHA-BETA	A,B	131,125	L,H	213,214
3H42	Crystal Structure Of PCSK9 In Complex With Fab From LDLR Competitive Antibody	Fab Mab1 W/ Proprotein Convertase Subtilisin/Kexin Type 9 (PCSK9)	A,B	126,540	L,H	217,238
3BSZ	Crystal Structure Of The Transthyretin-Retinol Binding Protein-Fab Complex	Fab Anti-Retinol-Binding Protein W/ Transthyretin-Retinol	A,E	127,176	L,H	215,215
3HI6	Crystal Structure Of Intermediate Affinity I Domain Of Integrin LFA-1 With The Fab Fragment Of Its Antibody AL-57	Fab AL-57 W/ Integrin LFA-1	A	180	L,H	212,220
2CMR	Crystal Structure Of The Hiv-1 Neutralizing Antibody D5 Fab Bound To The Gp41 Inner-Core Mimetic 5-Helix	Fab D5 W/ HIV GP41 Helix	A	226	L,H	208,217
3EFD	The Crystal Structure Of The Cytoplasmic Domain Of Kcsa	Fab W/ Kcsa	K	30	L,H	211,222
3NCY	X-Ray Crystal Structure Of An Arginine Agmatine Antiporter (Adic) In Complex With A Fab Fragment	Fab W/ Arginine Agmatine Antiporter	A	445	S,P	211,219

Table S4. Logistic regression coefficient, p-value and odds ratio of the significant physicochemical features.

Features	Coefficient	P-value	Odds ratio
ZEPII	9.05	2.27E-07	8518.537925
Buried surface area	-2.796	0.044027	0.06105379
Hydrogen bond density	-6.384	0.000824	0.001688356
Cation-pi density	2.066	0.047837	7.89318714

Table S5. The 20X20 amino acid propensity matrix. Paratope amino acids are indicated on the left side and epitope amino acids are indicated on the top side. The propensity data were generated using 84 non-redundant antigen-antibody complexes.

	ALA	ARG	ASN	ASP	CYS	GLU	GLN	GLY	HIS	ILE	LEU	LYS	MET	PHE	PRO	SER	THR	TRP	TYR	VAL
ALA	0.25	0.59	0.14	0.53	0	0.28	0.6	0.35	1.33	0.68	1.1	0.33	2.3	2.94	0.77	0.25	0.38	1.49	0.59	1
ARG	0.58	0.87	1.11	2.29	0	1.75	0.87	0.67	0.95	1.03	0.99	0.44	0.79	0.75	0.15	0.5	0.66	0.29	2.24	0.57
ASN	0.74	1.32	1.04	0.94	0.72	1.28	1.32	1.08	1.94	1.03	0.33	1.05	1.53	0.54	0.74	0.78	0.58	0.83	0.82	0.41
ASP	0.23	1.68	0.81	0.6	0	0.75	0.54	0.79	1.04	0.4	1.27	2.2	0.62	0.58	0.51	0.84	1.08	0.89	1.05	0.27
CYS	5.29	0	0	5.59	36.02	0	0	2.46	0	0	0	0	0	6.85	2.68	0	0	0	0	4.17
GLU	0.22	1.41	0.6	0.23	0	0.36	0.39	0.2	0.57	0.39	0.14	0.85	0.39	0.56	0.44	0.75	0.55	0.85	0.17	0.34
GLN	0.44	0.2	0.72	0.23	0	0.48	0.26	0.61	0	0.78	0.82	0.38	0	0.57	0.44	0.65	0.44	0	1.02	0
GLY	0.31	1.01	0.57	0.49	1.06	1.37	0.99	0.72	0.68	0.56	0.39	0.9	0.76	0.94	0.89	0.51	0.84	0.61	0.97	0.74
HIS	0.55	0.64	0.76	0.87	0	0.91	1.15	0.51	0.73	0.49	0.52	0.6	1	0	0.84	0.27	0.56	0	0.43	0.65
ILE	0.31	0.57	0.17	0.32	0	0.34	0.73	0.14	1.2	0.55	1.33	0.66	2.22	1.58	0.31	0.45	0.92	3	2.36	1.2
LEU	0.42	0.88	0.7	0.22	0.72	0.7	0.63	0.59	1.12	1.51	1.98	0.83	1.16	1.37	0.86	0.52	0.43	2.09	1.64	1
LYS	0	0.31	0.37	0.71	0	1.86	0.4	0.16	0.89	0	0.42	0.59	0	1.31	0.17	0.67	0.17	1.33	0	0.27
MET	0	0.99	1.17	0	0	1.17	0.64	0.5	1.4	0.95	0	0	3.88	0	0.54	0	0	2.1	1.65	0.84
PHE	1.81	1.36	0.74	0.72	0.77	0.87	1.22	1.16	2.98	0.81	1.41	1.17	0.82	2.05	1.49	0.67	1.03	1.78	0.35	1.6
PRO	0.75	1.04	0.41	0.2	0	0.41	1.12	0.17	1.97	1	1.4	0.49	2.72	1.94	0.38	0.55	0.57	0.74	1.16	0
SER	1.12	1.27	0.62	0.93	1.37	1.64	1.54	0.6	1.16	0.43	1.25	0.97	1.02	1.04	0.73	0.83	0.93	1.42	1.43	0.82
THR	0.84	1.17	0.79	1.14	0	1.06	1.15	0.34	1.42	0.54	0.37	0.83	1.31	0.16	0.79	0.77	1.03	0.24	0.56	0.76
TRP	1.27	1.71	1.16	1.05	3.37	0.47	2.03	0.99	2.61	0.51	1.06	1.78	1.03	0.73	1	1.12	0.86	0.56	1.86	1.56
TYR	1.48	2.21	1.83	1.56	2.04	1.96	1.6	1.73	2.01	1.9	2.38	1.78	1.89	2.69	1.88	1.35	1.21	1.4	1.36	1.46
VAL	0.3	1.1	0.49	0.78	1.01	1.3	0.88	0.28	1.56	0.79	1.11	0.26	0.54	1.15	0.3	0.59	0.45	2.92	0.69	0.47

Table S6. Mutations that increase EDIII-DV4 affinity while approximately maintaining affinity to EDIII of DV1-3.

Chain	CDR	Position	WT residue	Mutation
VH	H2	55	Ala	Glu
VH	H2	55	Ala	Asp
VL	L1	31	Arg	Lys
VL	L2	57	Asn	Glu
VL	L2	57	Asn	Ser
VL	L2	59	Glu	Gln
VL	L2	59	Glu	Asn
VL	L2	60	Ser	Trp
VL	L2	60	Ser	Tyr
VL	L2	60	Ser	Arg

Table S7. Predicted contacts made by affinity-enhancing mutations.

Chain & CDR	Position	WT residue	Mutation	Predicted DV4 contacts
VH – H2	55	Ala	Glu	H-bond, Ionic contact with Lys (310), Lys (323)
			Asp	H-bond, Ionic contact with Lys (310), Lys (323)
VL – L1	31	Arg	Lys	Ionic contact with Glu (311)
VL – L2	57	Asn	Glu	Ionic contact with Lys (305)
			Ser	H-bond with Lys (310)
VL – L2	59	Glu	Gln	H-bond with Glu (327)
			Asn	H-bond with Glu (327)
VL – L2	60	Ser	Trp	Hydrophobic contact with Ala (329)
			Tyr	H-bond with Glu (327)
			Arg	Ionic, H-bond with Glu (327) and H-bond with Gly (328)

Table S8. Affinities of single mutant antibodies with increased EDIII-DV4 affinity and similar affinities to EDIII of DV1-3 relative to 4E11 WT.

Mutation	CDR	EDIII-DV1 K_D (nM)	EDIII-DV2 K_D (nM)	EDIII-DV3 K_D (nM)	EDIII-DV4 K_D (nM)
4E11 WT	-	0.328	5.2	21.8	40,793
A55E	H2	0.295	0.323	2.95	4,442
R31K	L1	0.378	5.35	21.1	37,292
N57E	L2	0.281	1.75	33.9	8,408
E59Q	L2	0.772	10.8	102	11,034
S60W	L2	0.284	6.3	23.1	26,351

Table S9. Energetic calculations of 4E5A show mutations have additive effect on binding energy.

Antibody	EDIII-DV4 ΔG (kcal/mol)[a]	EDIII-DV4 ΔΔG (kcal/mol)[b]
4E11 WT	-5.98	---
VH-A55E	-7.29	-1.31
VL-R31K	-6.03	-0.05
VL-N57E	-6.92	-0.93
VL-E59Q	-6.76	-0.77
VL-S60W	-6.24	-0.26
4E5A	-9.59	-3.61

[a]Free energy calculated by $\Delta G = RT\ln(K_D)$ at 25°C

[b]$\Delta\Delta G = \Delta G_{mutant} - \Delta G_{WT}$

Table S10. Kinetic binding parameters for 4E11 and 4E5A measured by SPR.

	EDIII-DV1		EDIII-DV2		EDIII-DV3		EDIII-DV4	
	k_{on}[a]	k_{off}[b]	k_{on}[a]	k_{off}[b]	k_{on}[a]	k_{off}[b]	k_{on}[a]	k_{off}[b]
4E11	1.11	5.51	1.98	123	1.34	102	N.B.[c]	N.B.[c]
4E5A	1.17	20.8	2.01	14.1	2.76	143	0.766	875

[a]k_{on} values are expressed as ($x10^6$ $M^{-1}s^{-1}$)

[b]k_{off} values are expressed as ($x10^{-4}$ s^{-1})

[c]N.B., no binding

Table S11. Comparison of results of various *in silico* antibody affinity enhancement studies.

Study	Method	Antibody	Antigen	Crystal structure ?	Single /multiple antigen(s)	Affinity improvement (fold change)
Our study	Empirical informatics	4E11	DV E protein	No	Multiple (4)	~450
Lippow SM et. al., Nature Biotech (2007) (1)	Energetics	D44.1	lysozyme	Yes	Single	140, 10
Marvin J.S. et. al., Biochemistry (2003)(2)	Energetics	Y0101	VEGF	Yes	Single	~6
Clark LA et.al., Protein Science (2006)(3)	Energetics	AQC2	VLA1	Yes	Single (2)	~10
Farady et al. (2009) Bioorg. Med. Chem. Lett.(4)	Energetics	E2	Protease MT-SP1	Yes	Multiple	14

Table S12. Antibody mutations predicted with 'Calculate Mutation Energy (Binding)' protocol available on Discovery Studio. Mutations that increased the affinity of 4E11 are highlighted in yellow.

Mutation at ALA55	Mutation Energy	Effect of Mutation	Mutation at ARG31	Mutation Energy	Effect of Mutation	Mutation at ASN57	Mutation Energy	Effect of Mutation	Mutation at GLU59	Mutation Energy	Effect of Mutation	Mutation at SER60	Mutation Energy	Effect of Mutation
VH:ALA55			VL:ARG31			VL:ASN57			VL:GLU59			VL:SER60		
GLU	-1	stabilizing	LYS	-1.01	stabilizing	LEU	-1.79	stabilizing	PHE	-1.02	stabilizing	SER	-2.21	stabilizing
THR	-0.44	neutral	HIS	-0.13	neutral	PHE	-1.69	stabilizing	TYR	-1	stabilizing	PHE	-2.17	stabilizing
TRP	-0.4	neutral	MET	-0.04	neutral	TYR	-1.44	stabilizing	GLN	-0.86	stabilizing	ARG	-1.69	stabilizing
ASP	-0.37	neutral	PRO	-0.04	neutral	ARG	-0.88	stabilizing	ARG	-0.5	neutral	LYS	-1.69	stabilizing
GLN	-0.33	neutral	ARG	0	neutral	TRP	-0.64	stabilizing	LYS	-0.35	neutral	GLN	-1.65	stabilizing
LEU	-0.33	neutral	ILE	0.16	neutral	GLN	-0.62	stabilizing	ASP	-0.29	neutral	LEU	-1.44	stabilizing
TYR	-0.29	neutral	THR	0.22	neutral	MET	-0.57	stabilizing	MET	-0.24	neutral	TRP	-1.31	stabilizing
ARG	-0.23	neutral	VAL	0.22	neutral	HIS	-0.51	stabilizing	HIS	-0.23	neutral	MET	-1.26	stabilizing
PRO	-0.23	neutral	ASN	0.24	neutral	LYS	-0.04	neutral	LEU	-0.1	neutral	HIS	-0.8	stabilizing
ILE	-0.17	neutral	ALA	0.3	neutral	ASN	0	neutral	ILE	-0.01	neutral	ASN	-0.79	stabilizing
MET	-0.17	neutral	CYS	0.32	neutral	ILE	0.53	destabilizing	GLU	0	neutral	CYS	-0.64	stabilizing
VAL	-0.14	neutral	SER	0.34	neutral	ASP	0.58	destabilizing	PRO	0.05	neutral	THR	-0.57	stabilizing
PHE	-0.09	neutral	GLY	0.41	neutral	PRO	0.68	destabilizing	VAL	0.06	neutral	ALA	-0.56	stabilizing
CYS	-0.04	neutral	TYR	0.46	neutral	THR	0.93	destabilizing	THR	0.17	neutral	ASP	-0.45	neutral
ALA	0	neutral	PHE	0.47	neutral	CYS	1.14	destabilizing	SER	0.34	neutral	GLU	-0.42	neutral
HIS	0.06	neutral	GLN	0.48	neutral	GLU	1.17	destabilizing	CYS	0.39	neutral	GLY	-0.05	neutral
GLY	0.07	neutral	LEU	0.48	neutral	ALA	1.32	destabilizing	ALA	0.51	destabilizing	TYR	0	neutral
ASN	0.13	neutral	TRP	0.68	destabilizing	SER	1.53	destabilizing	GLY	0.52	destabilizing	ILE	0.43	neutral
SER	0.17	neutral	ASP	1.14	destabilizing	VAL	1.88	destabilizing	ASN	0.68	destabilizing	VAL	0.61	destabilizing
LYS	1.06	destabilizing	GLU	1.26	destabilizing	GLY	1.95	destabilizing	TRP	2.53	destabilizing	PRO	3.31	destabilizing

SI TEXT

SI Text1: Multivariate logistic regression: model fitting and diagnostics

Part I: Variable Transformation and Model Selection

First, we assess collinear features and those with missing values. We removed disulfide bridges due to missing value (none of the examined interfaces contains S-S bridge). Further, we removed aromatic-aromatic, aromatic-sulfur, hydrogen bonds (main chain-main chain, side chain-side chain, main chain-side chain), number of salt bridge interactions and number of hydrogen bonds that involve charged residues. The remaining features were standardized within each PDB with respect to the minimum value:

$$X_i' = \frac{(X_i - \min(X_i))}{\max(X_i) - min(X_i)}$$

Next we used stepwise selection method to search for proper models with minimum Akaike Information Criterion (AIC) criteria. Then, statistically insignificant features were removed. The selected model contains ZEPII (odds ratio = 4.94; p-value=2E-16), buried surface area (odds ratio = 0.59; p-value= 9.94E-04), density of hydrogen bonds (odds ratio = 0.40; p-value = 4.32E-07) and cation-pi interactions (odds ratio = 1.45; p-value = 8.31E-04) as the significant features.

Part II: Model Diagnostic

We checked the model with respect to the following aspects:

(a) Model adequacy:

We applied Chi-square test to check the adequacy of the model. The result shows that each of the features makes significant contribution to the model. If any one of the features is removed, the trimmed model is less predictive than the parent model.

(b) Goodness-of-Fit

The result of Hosmer and Lemeshow Goodness-of-Fit Test shows no evidence implying lack of fit. For all the ten equal-size subgroup, the expected number is very close to the observed number. The overall p-value of Chi-square test is 0.997.

(c) Independent variables collinearity;

We checked the collinearity diagnostic and found that all the condition indices are smaller than the benchmark (<10), indicating that there is no collinearity among the significant features.

(d) Model residuals performance.

For the fitted model, we calculated the Pearson residuals and deviation residuals and computed DFBETAS, DIFCHISQ, DIFDEV, RESCHI and RESDEV. For the cases where natural poses exist, a few of the fitted above indices are high (≈13 cases out of 40). However, the above diagnostics indicate that the model is generally good.

	Model adequacy	Hosmer and Lemeshow Goodness-of-Fit	Independent variables collinearity	Model residuals performance
RMSD=3	Y	0.347	Y	21/40
RMSD=5	Y	0.594	Y	13/40
RMSD=10	Y	0.763	Y	9/40

Note:

(1): "Y" indicates lack of collinearity.

(2): "Hosmer and Lemeshow Goodness-of-Fit" p-value

(3): "Model residuals performance" shows how many fitted point influence the model.

SI Text2: Homology modeling of 4E11 Fv

A structural model of 4E11 Fv was built using SIWW-MODEL homology modeling server (5). The solved crystal structure of 1A1D-2 (PDB: 2R29) (6), which has 86% and 85% sequence identities to 4E11 in VH and VL, was used as a template. The L2, L3, H1 and H2 CDR loops belong to canonical classes 1, 1, 1 and 2, respectively (7). L1 does not belong to any known canonical class. The length of CDR H3 loop is 7. No additional refinements were carried out.

SI Text3: Computational docking for generating 4E11-EDIII (DV 1-4) structures

The homology modeled 4E11 Fv was docked against EDIII of a select DV1 strain using ZDOCK. The choice to use DV1 antigen was influenced by the fact that mAb 4E11 was originally isolated from a mouse infected with a serotype 1 virus (8). The structure of the DV1 antigen was modeled using SWISS MODEL homology modeling server keeping the solved crystal structure of DV1 EDIII (PDB: 3IRC) as the template. ZDOCK uses shape complementarity along with desolvation and electrostatic energy terms ('ZRANK') to rank the docked poses (9). In order to ensure the docked poses do not deviate significantly from the native complex, mapped epitope and paratope residues found in the literature were forced to be included in the binding interface. Residues included in the interface were 307K, 389L and 391W (epitope; DV1 numbering as in 3IRC) and 101W, 102E (paratope; numbering based on sequence position).

The structures of 4E11 in complex with DV 2, 3, 4 (EDIII) were modeled using 4E11-DV1 EDIII structural model as the template. Backbone conformational changes upon antigen-antibody association are difficult to model computationally and were not attempted.

SI Text4: Cells & viruses

Vero (African green monkey kidney) and C6/36 (*Aedes albopictus*) cells were purchased from ATCC. Vero cells were cultured with DMEM/F-12 (50:50) medium (Invitrogen) supplemented with 10% FBS (Invitrogen) in a 37^{o}C humidified 5% CO_2 incubator. C6/36 cells

were maintained in EMEM (ATCC) supplemented with 10% FBS in a 28°C humidified 5% CO_2 incubator. Suspension Freestyle 293 cells (Invitrogen) were cultured in Freestyle 293 medium (Invitrogen). Dengue viruses TH-S-man (serotype 1), NGC (serotype 2), and H87 (serotype 3), and BC287/97 (serotype 4) were purchased from ATCC or BEI Resources. Viruses were propagated by infection of C6/36 cells (MOI ~0.1) and harvested after 5-8 days. Aliquots were stored at -80°C.

SI Text5: Focus forming assay

Viruses were titered by focus forming assay with Vero cells and expressed as focus-forming units (FFU) per ml. Serial dilutions of virus were incubated for 2 hours with 95% confluent Vero cells in 24-well plates at 37°C, after which one ml of viscous overlay (DMEM/F12 containing 1% Aquacide II [EMD Millipore]) was added to the monolayer. After 4-6 day incubation period at 37°C, the overlay was removed, cells were fixed with formalin, and foci were revealed by sequential incubation with pan-flavivirus 4G2 mouse antibody, HRP-conjugated goat anti-mouse IgG antibody (Santa Cruz Biotechnology), and TrueBlue Peroxidase Substrate (KPL).

SI Text6: Expression and purification of antibodies and EDIII proteins

4E11 antibody was generated by DNA synthesis of 4E11 VH and VL regions (GenBank accession numbers AJ131288.1 and AJ131289.1, respectively) and cloned using standard techniques into pcDNA 3.3 plasmid (Invitrogen) containing the constant region of either human IgG1 heavy chain or human kappa light chain. Mutant mAbs were generated by either site-directed mutagenesis (Agilent) or variable region DNA synthesis. Antibodies were expressed in Freestyle 293 cells by transient transfection with polyethyleneamine (PEI) and purified by protein A chromatography. EDIII DNA sequences (corresponding to E protein amino acid residues 293-400) of strains TH-S-man, NGC, H87, and BC298/97, representing serotypes 1-4, respectively, were synthesized with C-terminal 6X-His tags and cloned into pJExpress414 plasmids. The proteins were expressed in Origami2(DE3) *E. coli* (EMD Millipore), essentially as described(10). EDIII was purified by IMAC using His-Trap columns (GE Healthcare) and stored at 4°C or -20°C for long-term storage.

SUPPLEMENTARY REFERENCES

1. Lippow SM, Wittrup KD, & Tidor B (2007) Computational design of antibody-affinity improvement beyond in vivo maturation. (Translated from eng) *Nat Biotechnol* 25(10):1171-1176 (in eng).
2. Marvin JS & Lowman HB (2003) Redesigning an antibody fragment for faster association with its antigen. *Biochemistry* 42(23):7077-7083.
3. Clark LA*, et al.* (2006) Affinity enhancement of an in vivo matured therapeutic antibody using structure-based computational design. *Protein science : a publication of the Protein Society* 15(5):949-960.

4. Farady CJ, Sellers BD, Jacobson MP, & Craik CS (2009) Improving the species cross-reactivity of an antibody using computational design. *Bioorganic & medicinal chemistry letters* 19(14):3744-3747.
5. Schwede T, Kopp J, Guex N, & Peitsch MC (2003) SWISS-MODEL: An automated protein homology-modeling server. *Nucleic acids research* 31(13):3381-3385.
6. Lok SM*, et al.* (2008) Binding of a neutralizing antibody to dengue virus alters the arrangement of surface glycoproteins. *Nature structural & molecular biology* 15(3):312-317.
7. Chothia C*, et al.* (1989) Conformations of immunoglobulin hypervariable regions. *Nature* 342(6252):877-883.
8. Thullier P*, et al.* (1999) A recombinant Fab neutralizes dengue virus in vitro. *Journal of biotechnology* 69(2-3):183-190.
9. Pierce B & Weng Z (2007) ZRANK: reranking protein docking predictions with an optimized energy function. *Proteins* 67(4):1078-1086.
10. Saejung W*, et al.* (2006) Enhancement of recombinant soluble dengue virus 2 envelope domain III protein production in Escherichia coli trxB and gor double mutant. *Journal of Bioscience and Bioengineering* 102(4):333-339.